Electronic Supplementary Material (ESI) for Materials Chemistry Frontiers.

Electronic Supplementary Information

A helically-twisted ladder based on 9,9'-bifluorenylidene: synthesis, characterization, and carrier-transport property

Jinjia Xu,[a] Atsuro Takai,*[a] Alisa Bannaron,[a,b] Takafumi Nakagawa,[c] Yutaka Matsuo,[c] Manabu Sugimoto,[d] Yoshitaka Matsushita[a] and Masayuki Takeuchi*[a]

[a] *Molecular Design & Function Group, National Institute for Materials Science (NIMS), 1-2-1 Sengen, Tsukuba, Ibaraki 305-0047, Japan*

[b] *Institute for Materials Chemistry and Engineering, Kyushu University, 6-1 Kasuga-koen, Kasuga-city, Fukuoka 816-8580, Japan*

[c] *Department of Mechanical Engineering, School of Engineering, The University of Tokyo, 7-3-1 Hongo, Bunkyo-ku, Tokyo 113-8656, Japan*

[d] *Faculty of Advanced Science and Technology, Kumamoto University, 2-39-1 Kurokami, Chuo-ku, Kumamoto 860-8555, Japan*

Table of contents

Experimental section

General procedures. NMR spectra were recorded on a JEOL ECS-400 (400 MHz) spectrometer by using tetramethylsilane (0 ppm for ^{1}H NMR) as an internal standard. MALDI/TOF–MS measurements were performed on an AXIMA-CFR Plus (Shimadzu), with dithranol as a matrix. UV-vis absorption spectra were recorded on a JASCO V-670 spectrophotometer in a quartz cuvette of 1 cm path length. Absolute fluorescence quantum yield was recorded on a Hamamatsu absolute PL quantum yield spectrometer C11347. Cyclic voltammetry and differential pulse voltammetry were performed with an Eco Chemie AUTOLAB PGSTAT12 potentiostat in a deaerated CH_2Cl_2 containing 0.1 M $TBAPF_6$ as a supporting electrolyte at 298 K. A conventional three-electrode cell was used with a platinum working electrode and a platinum wire as a counter electrode. The redox potentials were measured with respect to an $Ag/AgNO_3$ (1.0×10^{-2} M) reference electrode. The oxidation potential of ferrocene as an external standard was 0.21 V (*vs.* $Ag/AgNO_3$) in CH_2Cl_2.

Quantum chemical calculation. Computational analysis and geometry optimization for **BF** and **CBF** in the ground state was performed using the Spartan'14 software or Gaussian 09, revision D.01 and Gauss View software program (version 5), respectively.[1] Molecular orbitals were obtained by B3LYP or M06-2X functional with the 6-31G** basis set. The excited states of **CBF** was studied using time-dependent DFT (TDDFT) method with the same DFT functional and the basis set.

Single crystal X-ray diffraction analysis. A single crystal of **CBF** was obtained by slow vapor diffusion of acetonitrile into a toluene solution of **CBF** at room temperature. All measurements were carried out using a Rigaku AFC11 Saturn724+ diffractometer at 213 K with Mo K_α radiation (λ = 0.71073Å). Cell refinement and data reduction were carried out by using the program d*trek package in the CrystalClear software suite.[2] Preliminary structures were solved using SHELXT[3] and refined by full-matrix least squares on F^2 using the SHELXL-2016[4] in WinGX program package.[5] All non-hydrogen atoms were refined anisotropically. The crystallographic data of **CBF** have been deposited with

Cambridge Crystallographic Data Centre as supplementary publication (CCDC 1590344 and 1817815). The pertinent crystallographic data are summarized in Table S1 and S2.

Space charge limited current (SCLC) measurements. Hole-only devices were fabricated with a configuration of glass/ITO/PEDOT:PSS/**CBF**/MoO_3/Al. PEDOT:PSS layers (30 nm-thick film) were formed on the glass/ITO substrate. A chlorobenzene solution of **CBF** was spin-coated, then MoO_3 (10 nm) and Al (100 nm) were deposited under vacuum sequentially. The electron-only device configuration was glass/Al/**CBF**/LiF/Al. After the spin-coating of **CBF** in chlorobenzene, LiF (0.6 nm) and Al (100 nm) were deposited under vacuum. Similarly, devices were also prepared by replacing **CBF** with **BF**. *J–V* curves of these devices were measured with a sweeping voltage using a Keithley 2400 source meter unit. The film thicknesses (50 nm for **CBF** and 100 nm for **BF**) represent average values of at least three measurements, which were determined by using a Dektak 6M stylus profiler. The career mobilities can be obtained from the fitting of the *J–V* curves with a following equation;

$$J = 9/8\ \varepsilon_0 \bullet \varepsilon_r\ \mu\ V^2/L^3$$

where J is the current density, ε_0 is the permittivity of free space, ε_r is the relative permittivity of the material, μ is the mobility, V is the effective voltage, and L is the thickness of the active layer.

Materials. All chemicals were purchased from Sigma-Aldrich, Tokyo Chemical Industry, Kanto Chemical, or Wako Pure Chemical Industries and used unless otherwise noted. Ferrocene and tetrabutylammonium hexafluorophosphate ($TBAPF_6$) were purified according to the literature.[6] Key compounds were purified by a recycling preparative HPLC (ChromNAV system equipped with a PU-2086 Plus pump and a RI-2031 Plus detector, JASCO Corporation) equipped with gel permeation chromatography (GPC) columns (YMC-GPC T4000). Air and water sensitive synthetic manipulations were performed under an argon atmosphere using standard Schlenk techniques. Pristine 9,9'-bifluorenylidene (**BF**) is commercially available from Wako Pure Chemical Industries.

Synthesis of 1.

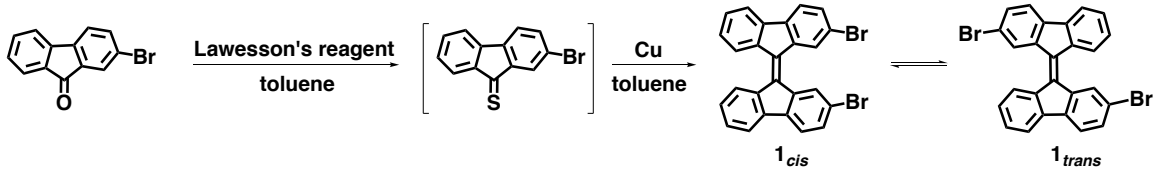

The precursor 2-bromo-9-fluorenone (500 mg, 1.93 mmol) and Lawesson's reagent (576 mg, 1.43 mmol) were refluxed under Ar atmosphere in anhydrous toluene (30 mL). The orange solution gradually turned to red one during the stirring overnight. A catalytic amount of copper powder (12.4 mg, 0.1 mmol) was then added to the reaction mixture. The mixture was kept refluxing for 3 h, allowed to cool down to room temperature, and got through the silica gel pad to remove the copper. The mixture was further washed with water, brine, and aqueous K_2CO_3. The combined organic layers were extracted with $CHCl_3$ for three times, dried over anhydrous $MgSO_4$, and the solvent was evaporated under reduced pressure. The crude product was purified by column chromatography (silica gel) with hexane/$CHCl_3$ (5:1) as the eluents and by recrystallization from $CHCl_3$ and hexane to afford an orange powder as a mixture of $\mathbf{1}_{cis}$ and $\mathbf{1}_{trans}$ (110 mg, 12%). ^{1}H NMR ($CDCl_3$, 400 MHz, 298 K): δ (ppm) 7.21–7.30 (m, 24H), 7.33–7.38 (m, 3H), 7.45–7.48 (m, 3H), 7.56 (dd, 3H, J = 8 Hz), 7.67 (dd, 3H, J = 8 Hz), 8.28 (d, 2H, J = 8 Hz, $\mathbf{1}_{trans}$), 8.34 (d, 1.5H, J = 8 Hz, $\mathbf{1}_{cis}$), 8.43 (d, 1.5H, J = 1.2 Hz, $\mathbf{1}_{cis}$), 8.47 (d, 2H, J = 1.2 Hz, $\mathbf{1}_{trans}$). ^{13}C NMR ($CDCl_3$, 100 MHz, 298 K): δ (ppm) 120.07, 120.14, 120.68, 120.74, 121.16, 121.19, 126.63, 126.72, 127.36, 127.51, 129.16, 129.42, 129.80, 129.82, 132.11, 137.63, 137.71, 139.53, 139.72, 140.07, 140.10, 140.53, 140.60, 140.78, 140.82.

Synthesis of CBF.

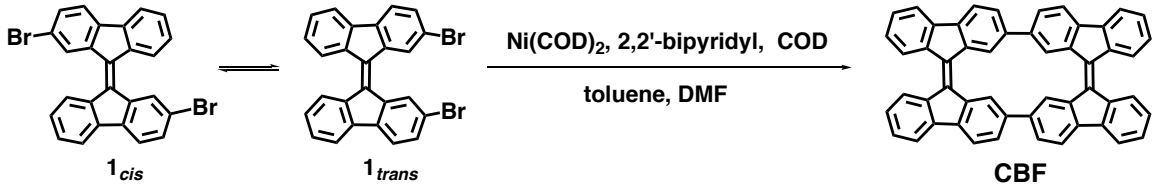

Compound **1** (200 mg, 0.411 mmol) as a mixture of $\mathbf{1}_{cis}$ and $\mathbf{1}_{trans}$ in 3:4 ratio, bis(1,5-cyclooctadiene)nickel(0): $Ni(COD)_2$ (237 mg, 0.658 mmol), 2,2'-bipyridyl (120 mg, 0.658 mmol) were placed in a flask under Ar atmosphere. A solution of COD (71.2 mg, 0.658 mmol) in DMF (3 mL) and toluene (15 mL) was added, and the reaction mixture was stirred at 90 °C for 48 h. After cooling down to room temperature, the mixture was got through the silica gel pad to remove the catalyst and then diluted with $CHCl_3$. The organic layer was washed with a saturated aqueous EDTA solution and a 3 M HCl aqueous solution, respectively. The combined organic layers were washed with brine and dried over anhydrous $MgSO_4$. The solvent was removed by evaporation under reduced pressure. The crude product was purified by column chromatography (silica gel) with hexane/$CHCl_3$ (3:1) as the eluents and by recycling GPC to afford a red powder (50 mg, 19%). ^{1}H NMR (CD_2Cl_2, 400 MHz, 298 K): δ (ppm) 7.17–7.21 (t, 4H, J = 8 Hz), 7.32–7.36 (t, 4H, J = 8 Hz), 7.44–7.46 (d, 4H, J = 8 Hz), 7.70–7.75 (m, 8H), 8.39–8.41 (d, 4H, J = 8 Hz), 8.79 (s, 4H). ^{13}C NMR (CD_2Cl_2, 100 MHz, 298 K): δ (ppm) 118.96, 119.03, 125.83, 126.00, 126.61, 128.08, 128.54, 137.68, 137.68, 139.41, 140.36, 140.37, 141.17. MALDI/TOF–MS: m/z calcd 652.2; found 651.7.

Supporting data

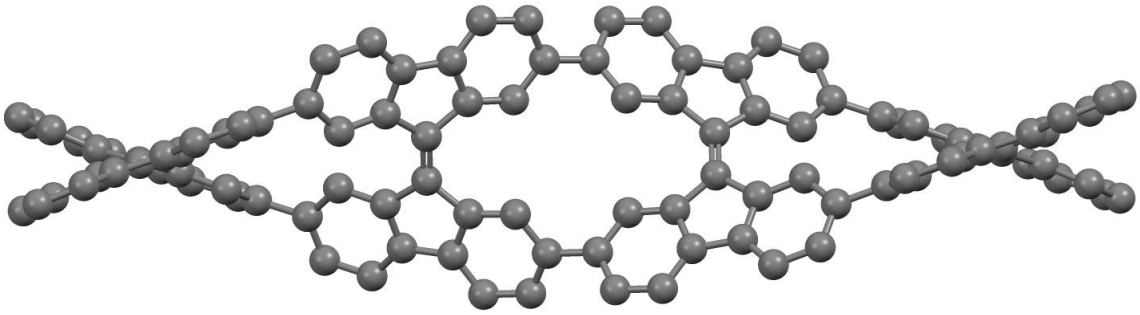

Fig. S1 Optimized structure of a plausible **BF**-based ladder oligomer (tetramer) calculated by DFT at the B3LYP/6-31G** level. Hydrogen atoms are omitted for clarity. The torsional angles around the central C=C bonds are (from left to right) 32.8°, 30.6°, 30.6°, and 32.8°, respectively.

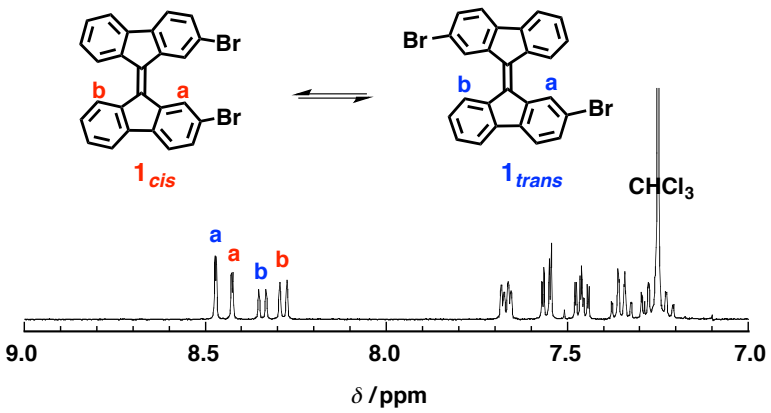

Fig. S2 ^{1}H NMR spectrum of **1** in $CDCl_3$ at 298 K. The ratio between $\mathbf{1}_{cis}$ and $\mathbf{1}_{trans}$ was determined by the integration values of H_a and H_b. The ratio between the integration values of H_a and H_b is $K = [\mathbf{1}_{trans}]/[\mathbf{1}_{cis}] = 4/3$. Given the standard Gibbs energy changes from $\mathbf{1}_{cis}$ to $\mathbf{1}_{trans}$ as $\Delta G = -RT\ln K$, where R (J K^{-1} mol^{-1}) is the gas constant and T (K) is the absolute temperature, ΔG is determined to be –0.71 kJ mol^{-1} at 298 K.

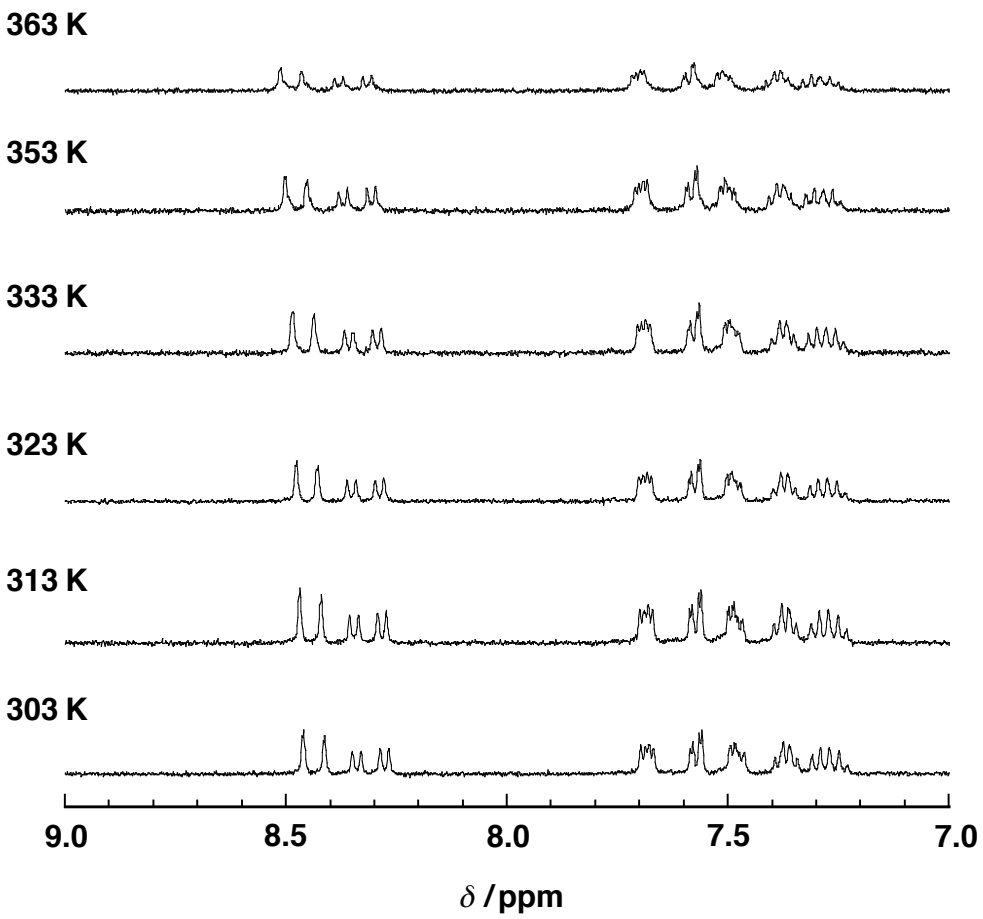

Fig. S3 Variable-temperature ^{1}H NMR spectra of **1** in 1,1,2,2-tetrachloroethane-d_2.

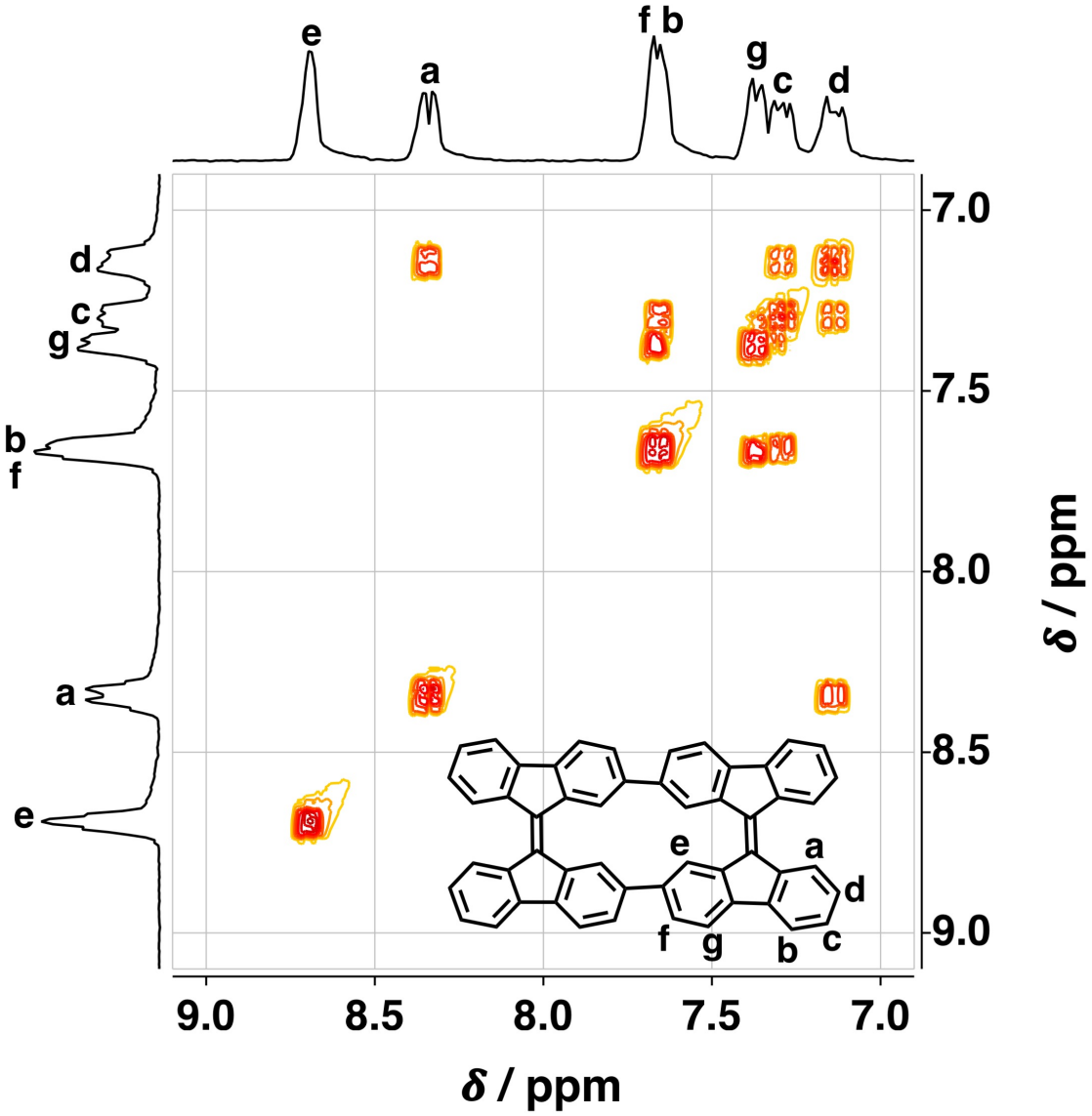

Fig. S4 2D $^{1}H,^{1}H$ COSY NMR spectrum of **CBF** (400 MHz, in CD_2Cl_2) at 298 K.

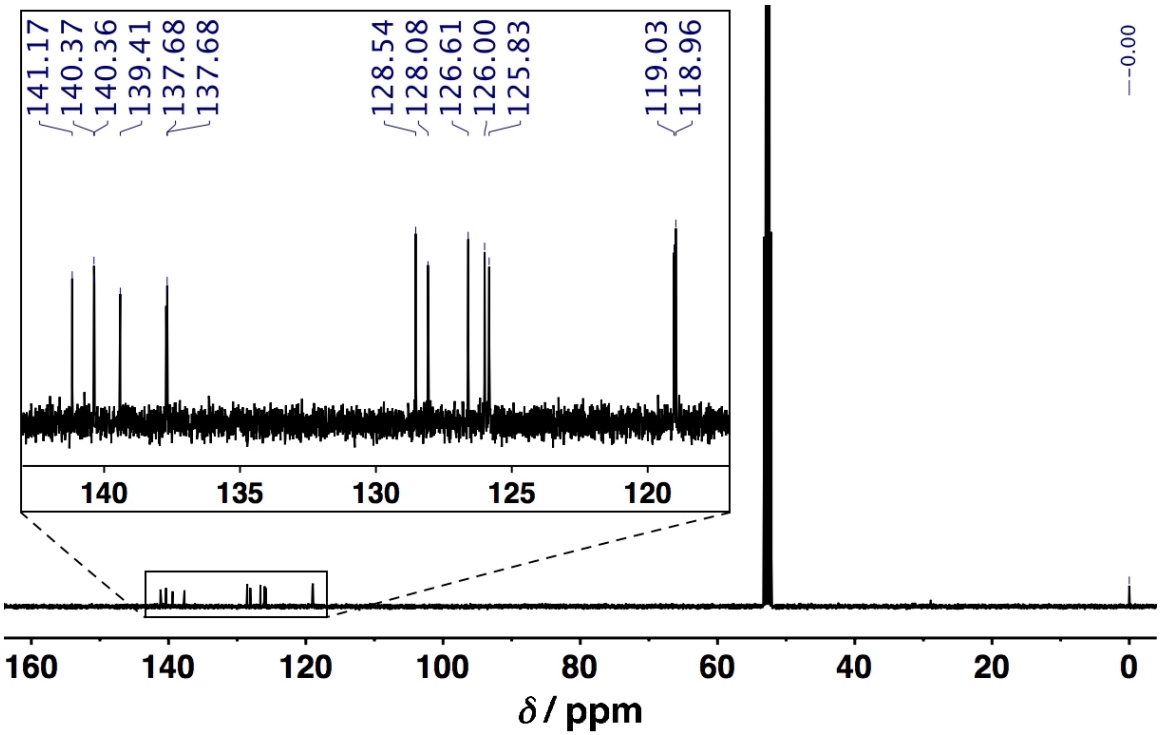

Fig. S5 ^{13}C NMR spectrum of **CBF** (100 MHz, in CD_2Cl_2) at 298 K.

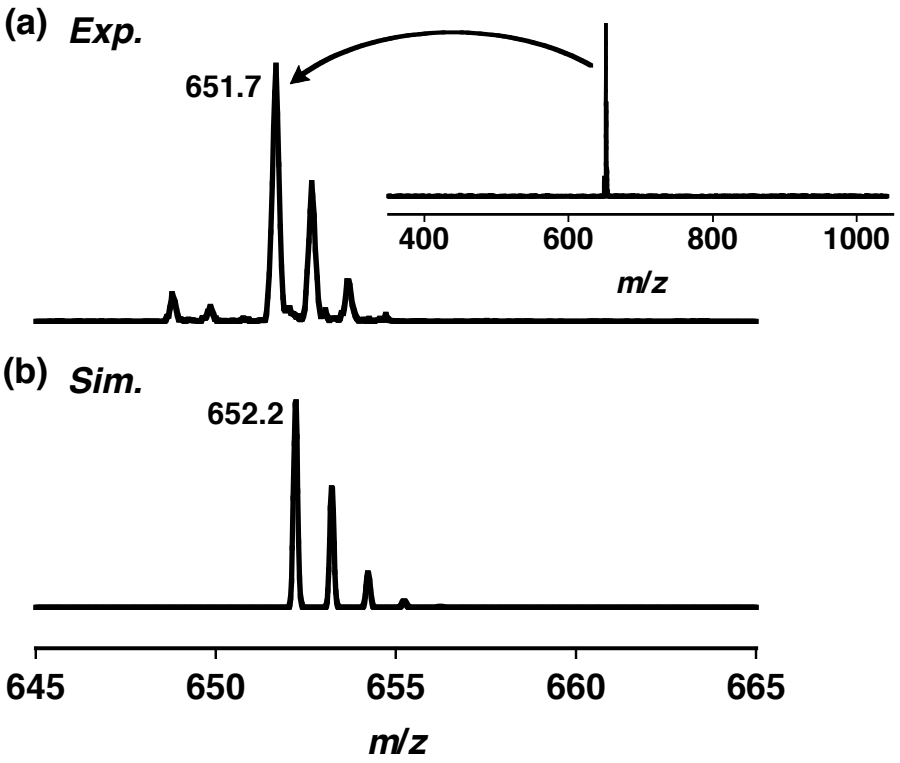

Fig. S6 (a) MALDI/TOF–MS (negative ion, linear mode) of **CBF** and (b) the calculated isotopic distribution for **CBF** (calcd for $C_{52}H_{28}$).

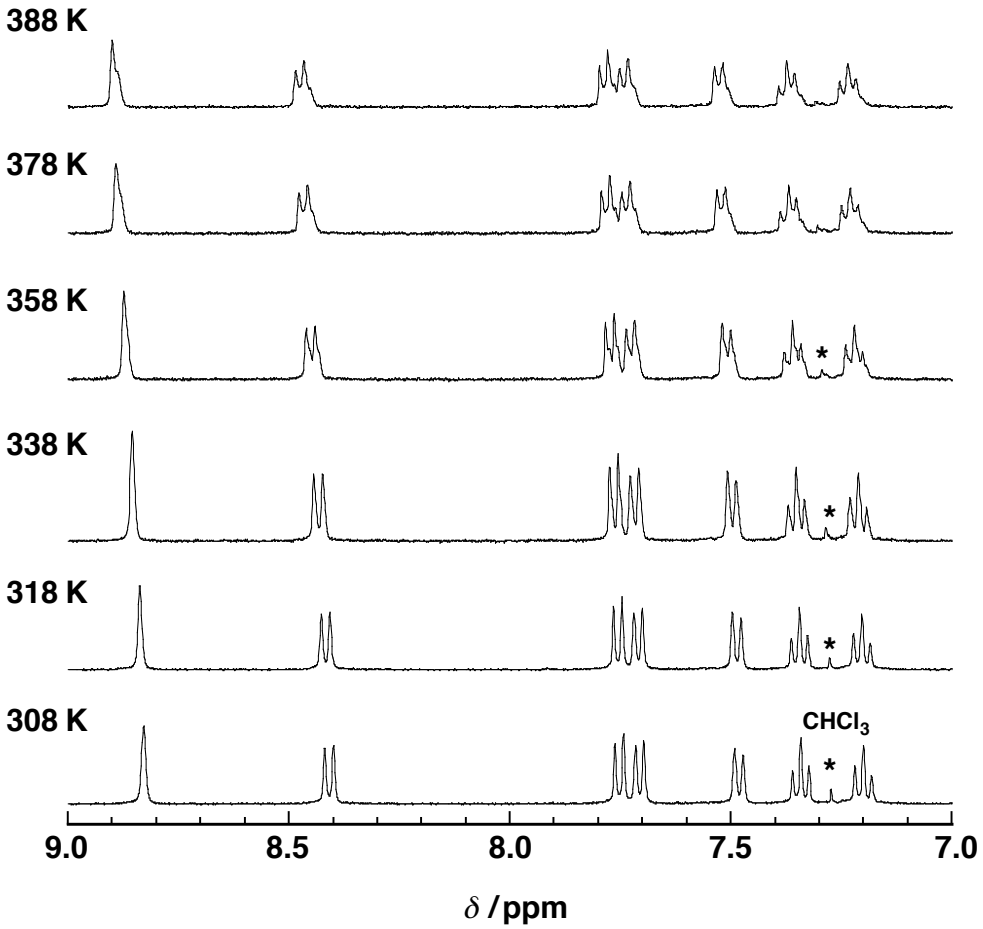

Fig. S7 Variable-temperature ^{1}H NMR spectra of **CBF** in 1,1,2,2-tetrachloroethane-d_2.

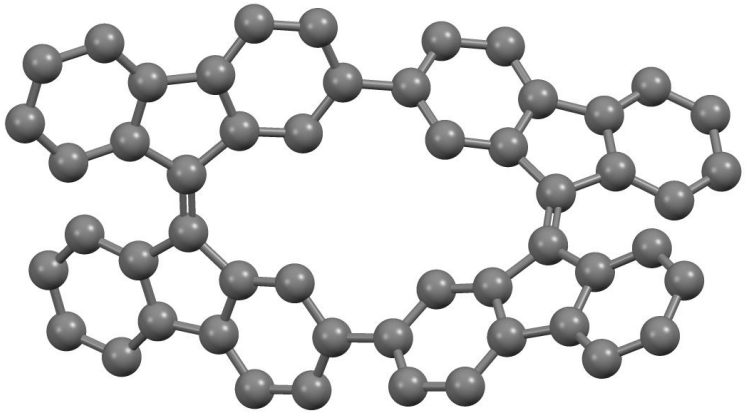

Fig. S8 Optimized structure of **CBF** calculated by DFT at the B3LYP/6-31G** level. Hydrogen atoms are omitted for clarity.

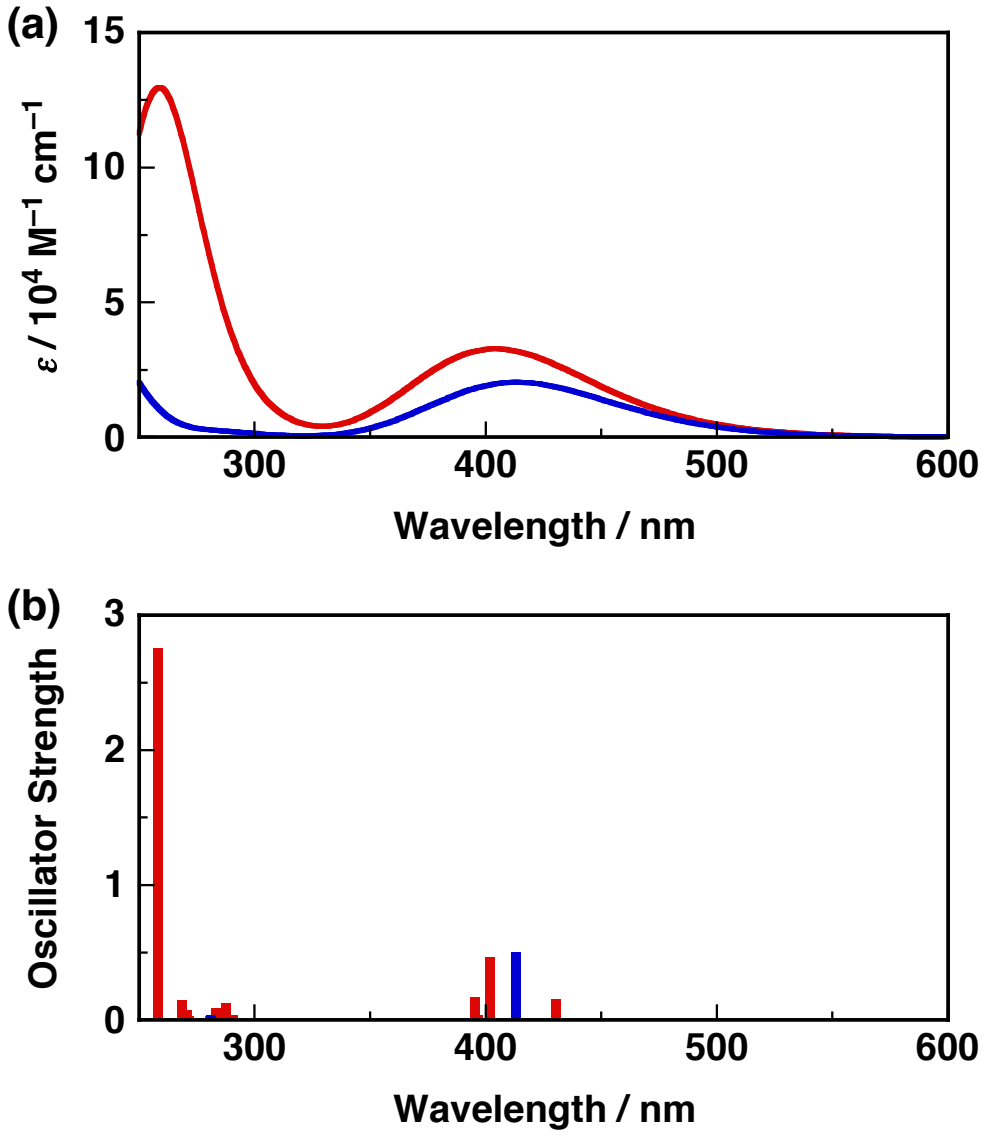

Fig. S9 (a) Predicted UV-vis spectra of **CBF** (red line) and **BF** (blue line), and (b) their oscillator strengths calculated by TDDFT at the M06-2X/6-31G** level.

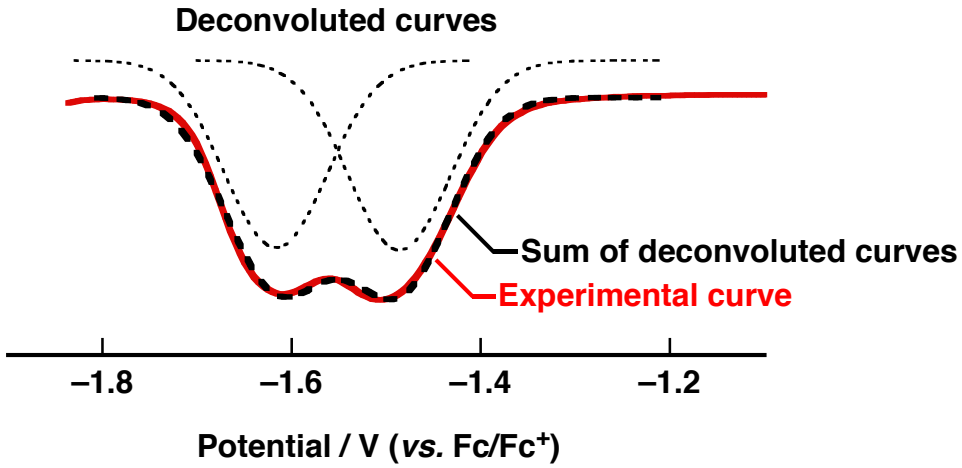

Fig. S10 DPV (red line) of **CBF** in deaerated CH_2Cl_2 containing 0.1 M $TBAPF_6$ with the scan rate of 100 mV s^{-1}. Two reduction potentials at –1.49 V and –1.62 V were obtained with a ratio of current intensity of 1:1 by Gaussian simulation (dashed lines).

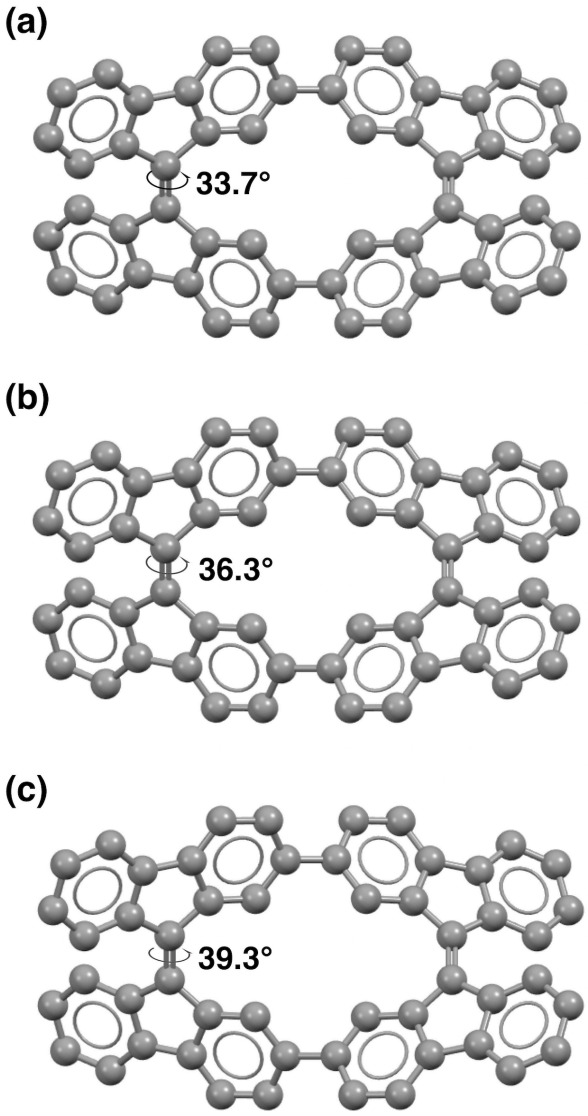

Fig. S11 Optimized structures of (a) **CBF**, (b) **CBF**$^{\bullet-}$ and (c) **CBF**$^{2-}$ and the torsional angles around the central carbon–carbon double bonds obtained by DFT calculations.

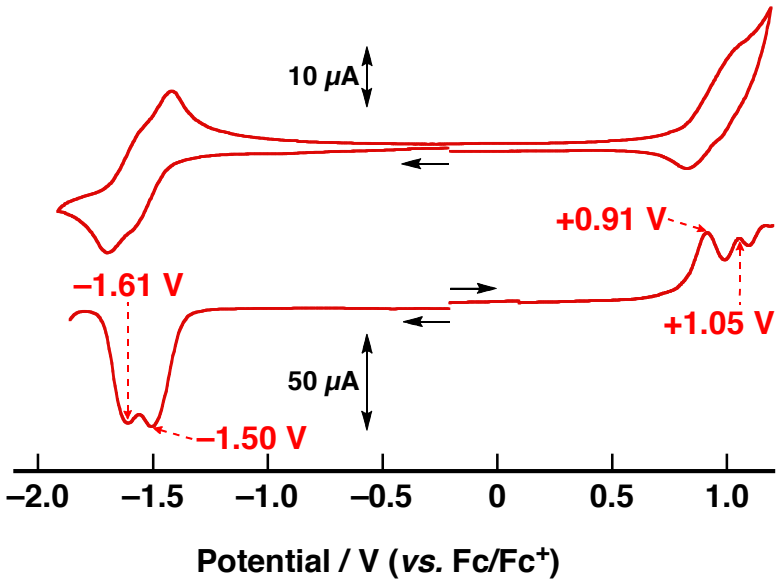

Fig. S12 CV (top) and DPV (bottom) of **CBF** in deaerated CH_2Cl_2 (0.5 mM) containing 0.1 M $TBAPF_6$ with the scan rate of 50 mV s^{-1}.

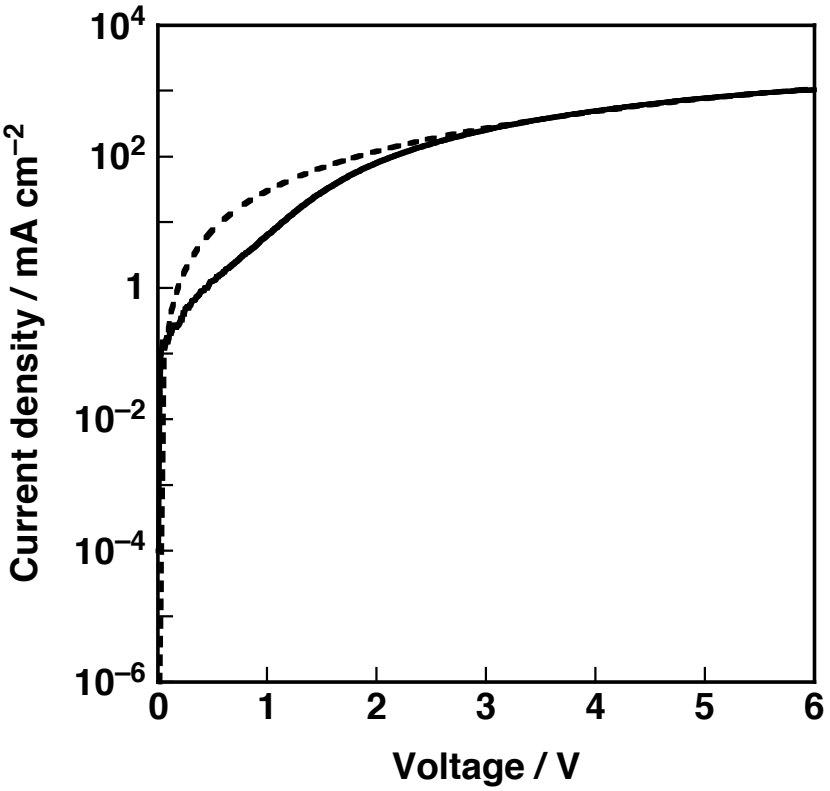

Fig. S13 SCLC chart of **CBF** for hole transport (solid line) with a fitting curve (dashed line, R^2 value of 0.995). Device configurations are glass/ITO/PEDOT:PSS/**CBF**/MoO_3/Al.

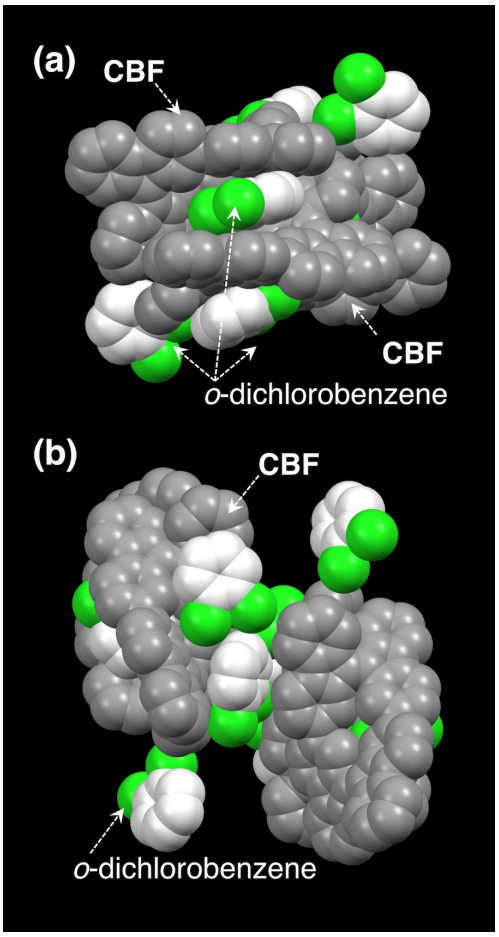

Fig. S14 Crystal packing structure of **CBF** grown in an *o*-dichlorobenzene solution: (a) side view and (b) top view. Hydrogen atoms are omitted for clarity. The pertinent crystallographic data are summarized in Table S2.

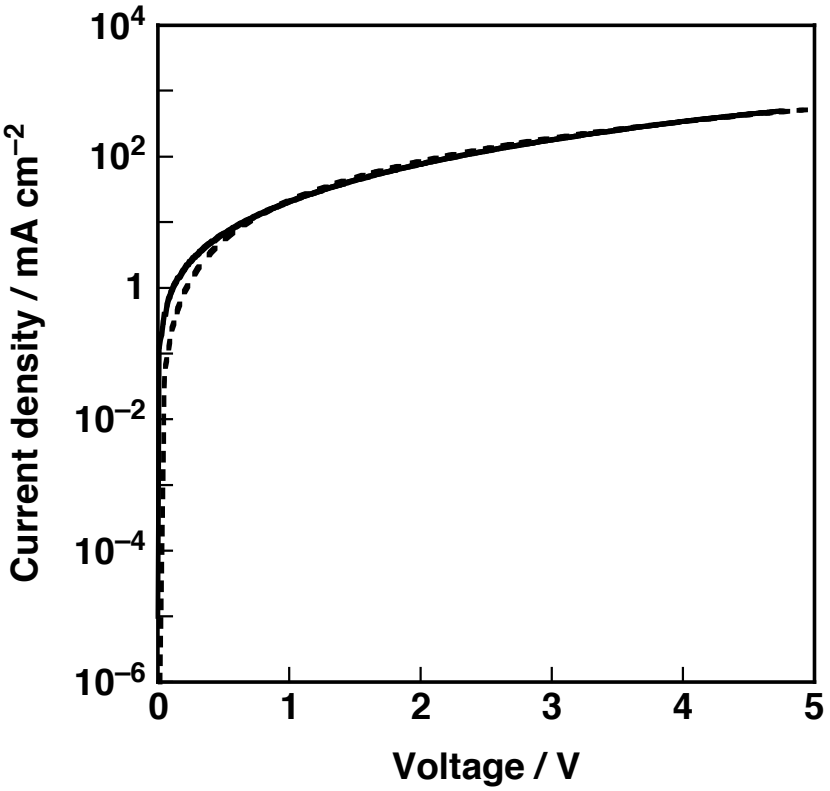

Fig. S15 SCLC chart of **BF** for hole transport (solid line) with a fitting curve (dashed line, R^2 value of 0.997). Device configurations are glass/ITO/PEDOT:PSS/**BF**/MoO_3/Al.

Table S1 X-ray crystallographic data for **CBF**

formula	$C_{52}H_{28}$
formula weight (fw)	652.78
crystal system	tetragonal
space group	*P*-4c2
T / K	213(2)
a / Å	14.367(4)
b / Å	14.367(4)
c / Å	7.992(3)
α / deg.	90
β / deg.	90
γ / deg.	90
V / Å^3	1649.6(11)
Z	8
D_x / g cm^{-3}	1.314
μ / mm^{-1}	0.075
measured reflections	5308
independent reflections	886
observed reflections	859 with $I > 2.0\sigma(I)$
parameters refined	120
$R1$ ($I > 2.0\sigma(I)$)	0.0469
$wR2$ (all data)	0.1067
GOF	1.299
CCDC	1590344

Table S2 X-ray crystallographic data for **CBF** including two *o*-dichlorobenzene molecules

formula	$C_{52}H_{28}$, $(C_6H_4Cl_2)_2$
formula weight (fw)	946.73
crystal system	monoclinic
space group	$P2_1/c$
T / K	113(2)
a / Å	18.181(2)
b / Å	12.6500(16)
c / Å	19.801(2)
α / deg.	90
β / deg.	96.169(3)
γ / deg.	90
V / Å^3	4527.5(10)
Z	4
D_x / g cm^{-3}	1.389
μ / mm^{-1}	0.307
measured reflections	12773
independent reflections	3943
observed reflections	2929 with $I > 2.0\sigma(I)$
parameters refined	613
$R1$ ($I > 2.0\sigma(I)$)	0.0382
$wR2$ (all data)	0.1363
GOF	1.113
CCDC	1817815

References

1 (*a*) M. J. Frisch, G. W. Trucks, H. B. Schlegel, G. E. Scuseria, M. A. Robb, J. R. Cheeseman, G. Scalmani, V. Barone, G. A. Petersson, H. Nakatsuji, X. Li, M. Caricato, A. Marenich, J. Bloino, B. G. Janesko, R. Gomperts, B. Mennucci, H. P. Hratchian, J. V. Ortiz, A. F. Izmaylov, J. L. Sonnenberg, D. Williams-Young, F. Ding, F. Lipparini, F. Egidi, J. Goings, B. Peng, A. Petrone, T. Henderson, D. Ranasinghe, V. G. Zakrzewski, J. Gao, N. Rega, G. Zheng, W. Liang, M. Hada, M. Ehara, K. Toyota, R. Fukuda, J. Hasegawa, M. Ishida, T. Nakajima, Y. Honda, O. Kitao, H. Nakai, T. Vreven, K. Throssell, J. A. Montgomery, Jr., J. E. Peralta, F. Ogliaro, M. Bearpark, J. J. Heyd, E. Brothers, K. N. Kudin, V. N. Staroverov, T. Keith, R. Kobayashi, J. Normand, K. Raghavachari, A. Rendell, J. C. Burant, S. S. Iyengar, J. Tomasi, M. Cossi, J. M. Millam, M. Klene, C. Adamo, R. Cammi, J. W. Ochterski, R. L. Martin, K. Morokuma, O. Farkas, J. B. Foresman and D. J. Fox, *Gaussian 09, Revision D.01*, Gaussian, Inc., Wallingford, Connecticut, 2016; (*b*) R. Dennington, T. Keith and J. Millam, *GaussView, Version 5*, Semichem Inc., Shawnee Mission, Kansas, 2009.

2 *CrystalClear*, Rigaku Corporation, Akishima, Tokyo, 2005.

3 G. M. Sheldrick, *Acta Crystallogr., Sect. A: Found. Adv.*, 2015, **71**, 3.

4 G. M. Sheldrick, *Acta Crystallogr., Sect. C: Struct. Chem.*, 2015, **71**, 3.

5 L. J. Farrugia, *J. Appl. Crystallogr.*, 1999, **32**, 837.

6 W. L. F. Armarego and C. L. L. Chai, *Purification of Laboratory Chemicals,* Elsevier Inc., Oxford, 6th edition, 2009.